Food Chemistry 358 (2021) 129884

Contents lists available at ScienceDirect

Food Chemistry

journal homepage: www.elsevier.com/locate/foodchem

Interaction pattern of histidine, carnosine and histamine with methylglyoxal and other carbonyl compounds

Raheleh Ghassem Zadeh, Varoujan Yaylayan *

McGill University, Department of Food Science and Agricultural Cshemistry, 21111 Lakeshore, Ste. Anne de Bellevue, Quebec, Canada

ARTICLE INFO

Keywords:
Histidine
Histamine
1,2-Dicarbonyl compounds
[U-$^{13}C_6$]Glucose
Methylglyoxal
Glyoxal
PhIP
Scavenging activity
Isotope labeling technique
ESI-qTOF-MS/MS

ABSTRACT

The ability of histidine to scavenge sugar-derived 1,2-dicarbonyl compounds was investigated using aqueous methanolic model systems containing histidine or histamine in the presence of glucose, methylglyoxal, or glyoxal. The samples were prepared either at room temperature (RT) or at 150 °C and analyzed using ESI-qTOF-MS/MS and isotope labeling technique. Replacing glucose with [U-$^{13}C_6$]glucose allowed the identification of glucose carbon atoms incorporated in the products. Various sugar-generated carbonyl compounds ranging in size from C1 to C6 were captured by histidine or histamine. The majority of the fragments incorporated were either C3 or C2 units originating from glyoxal (C2) or methylglyoxal (C3). The ESI-qTOF-MS/MS analysis indicated that histamine could react with either of the two carbonyl carbons of methylglyoxal utilizing the α-amino group and/or the imidazolium moiety. Furthermore, when histidine was added to 2-amino-1-methyl-6-phenylimidazo(4,5-*b*)pyridine (PhIP) generating model system, it completely suppressed the formation of PhIP due to scavenging of phenylacetaldehyde.

1. Introduction

Numerous scavenging agents such as pyridoxamine (Booth et al., 1996), creatine (Löbner et al., 2015), flavonoids (Procházková et al., 2011), and aminoguanidine (Hirsch et al., 1992) have been proposed in the past to mitigate the harmful effects of thermally generated reactive 1,2-dicarbonyl species formed during food processing (Hellwig et al., 2018). Recently, we have introduced the concept of in situ generation of carbonyl scavenging agents during thermal processing of food from selected amino acids such as tryptophan (Ghassem Zadeh & Yaylayan, 2019). The main scavenging agent generated from thermal degradation of tryptophan was identified to be indole. Indole was shown to undergo electrophilic aromatic substitution type reactions with carbonyl compounds at positions 2 and 3 and, hence scavenge more than one mole of carbonyl compound per mole of indole. It was further demonstrated that indole was able to trap the reactive 1,2-dicarbonyl compounds at room temperature as well as at higher temperatures of food processing (Zadeh & Yaylayan, 2020a, 2020b). Histidine, on the other hand, has been shown to be an efficient anti-crosslinking agent along with carnosine (a histidine-containing dipeptide) when incubated at 37 °C for 2 days in the presence of glyceraldehyde. Electrophoretic analysis showed a greater protective role of histidine than carnosine through its scavenging ability of the reactive glycating agents via both primary amino moiety and imidazolium group (Hobart et al., 2004). Furthermore, in vivo and in vitro investigations demonstrated the ability of carnosine to reduce Advanced glycation end products (AGE) generation via reaction with reducing sugars or other reactive species (such as lipid peroxidation intermediates) (Freund et al., 2018). The reaction between lipid peroxidation products, in particular, α βnsaturated aldehydes such as malondialdehyde (MDA), acrolein or 4-hydroxynonenal (HNE), and histidine or histidine-containing dipeptides have been also investigated (Guiotto et al., 2005; Vistoli et al., 2017; Xie et al., 2013). In addition, the reactivity of histidine with reducing sugars was also studied under the food processing conditions (Gi & Baltes, 1995, 1993a, 1993b, 2005) and various volatile reaction products such as 2-acetyl- and 2-propionyl-pyrido[3,4-*d*]imidazole derivatives were identified in the model systems and in food products, using GC/MS analysis (Gi & Baltes, 1995, 1993b, 2005). Similar to tryptophan, these studies have confirmed the ability of the initial Schiff base formed between histidine and carbonyl compounds to undergo Pictet-Spengler type reaction and subsequently form volatile pyrido[3,4-*d*]imidazole derivatives. However, the nature of non-volatile reaction products generated at high temperatures when histidine derivatives were reacted with carbohydrate-derived carbonyl compounds such as methylglyoxal has not been identified. Considering

* Corresponding author.
E-mail address: Varoujan.yaylayan@mcgill.ca (V. Yaylayan).

https://doi.org/10.1016/j.foodchem.2021.129884
Received 18 January 2021; Received in revised form 18 March 2021; Accepted 27 March 2021
Available online 20 April 2021

the crucial role of these carbonyl moieties in vivo and in vitro, understanding the chemical pathways through which histidine can scavenge these reactive precursors during the processing of foods may provide promising insight into their application strategies.

2. Experimental procedures

2.1. Materials & reagents

L-carnosine (99%), L-histidine (98%), histamine (97%), methylglyoxal (40% MG solution in water) (≥97%), glyoxal trimeric dihydrate (GO) (≥97%), methanol (99%) and D-glucose (Glc) were purchased from Sigma-Aldrich chemical company (Milwaukee, WI). The [U-$^{13}C_6$]D-glucose (99%) and [3-^{13}C]L-phenylalanine (99%) were purchased from Cambridge Isotope Laboratories (Tewksbury, MA, USA). 2-Amino-1-methyl-6-phenylimidazo[4,5-*b*]pyridine (PhIP) was obtained from Toronto Research Chemicals Inc. (Toronto, Ontario, Canada). Reactions were performed in sealed stainless-steel reactors heated in a commercial toaster oven (1200 Watts).

2.2. Preparation of model systems

L-carnosine (9.4 mg), L-Histidine (6.5 mg), or histamine (4.5 mg) were dissolved in methanol/water (50:50), subsequently, the 1,2-dicarbonyl compound was added to the solution and mixed. Model systems (see Table 1) prepared at 1:1 M ratio or 1:2 M ratio with excess 1,2-dicarbonyl in methanol/water (50:50) solution, and either heated at 150 C for 1.5 h in stainless-steel reactors or were kept in closed glass vials at RT for a week. Similarly, model systems consist of histidine or histamine with glucose and [U-$^{13}C_6$]glucose were prepared in methanol/water at 1:1 M ratio and heated at 150 C for 1.5 h in a stainless-steel reactor. In addition, either histidine or histamine was dissolved in methanol/water (50:50), then phenylacetaldehyde at 1:1 and 1:2 M ratio was added to the solution, mixed, and heated in the reactor at 150 C for 1.5 h. The reaction mixtures were subsequently analyzed by ESI-qTOF-MS/MS analysis. All samples were prepared and analyzed in two replicates.

2.3. Scavenging of phenylacetaldehyde by histidine or histamine in the PhIP generating model system

A PhIP generating model system consisting of creatinine/serine/phenylalanine (Ghassem Zadeh & Yaylayan, 2019) in a 1:1:1 M ratio was prepared and tested for its ability to generate PhIP the most abundant carcinogenic heterocyclic amines in cooked meat. To confirm the scavenging efficacy of histidine towards phenylacetaldehyde, an important precursor of PhIP; histidine or histamine were added to the above reaction mixture before heating and analyzed for the presence of PhIP and for the formation of histamine-phenylacetaldehyde adducts. Furthermore, phenylalanine was replaced with [3-^{13}C]phenylalanine in the PhIP generating model system and subsequently analyzed using qTOF-MS/MS after heating in water/methanol at 220C for 2 h. All samples were analyzed in at least two replicates.

Table 1
Composition of the model systems.[a]

Unlabeled Model systems	Isotopic labeled counterparts containing Model systems
Carnosine/methylglyoxal (1:1) & (1:2)[b]	Histidine/[U-$^{13}C_6$]Glc (1:1)[b]
Histidine/methylglyoxal (1:2)[b&d]	Histamine/[U-$^{13}C_6$]Glc (1:1)[b]
Histamine/methylglyoxal (1:2) [b&d]	Creatinine/serine/[^{13}C-3]phenylalanine/histidine (1:1:1:1)[c]
Carnosine/GO (1:1)[b]	Creatinine/serine/[^{13}C-3]phenylalanine/histamine (1:1:1:1)[c]
Histidine/GO (1:1) [b&d]	
Histamine/GO (1:1) [b&d]	
Histidine/Glc (1:1)[b]	
Histamine/Glc (1:1)[b]	
Histidine/paraformaldehyde (1:1)[b]	
Histamine/paraformaldehyde (1:1)[b]	
Histidine/phenylacetaldehyde (1:1) & (1:2)[b]	
Histamine/phenylacetaldehyde (1:1)[b]	
Creatinine/serine/phenylalanine (1:1:1)[c]	
Creatinine/serine/phenylalanine/histidine (1:1:1:1)[c]	
Creatinine/serine/phenylalanine/histamine (1:1:1:1)[c]	

2.4. Electrospray ionization/ quadrupole time of flight/ mass spectrometric analysis (ESI/qTOF/MS)

The samples were diluted in methanol (90% v/v) before analyzing by ESI/qTOF/MS. The system used was a Bruker Maxis Impact quadrupole time-of-flight mass spectrometer (Bruker Daltonics, Bremen, Germany) operating in positive ion mode. Calibration of the instrument was carried out by using sodium formate clusters. The diluted samples were infused continuously into the detector. The acquisition parameters for electrospray interface were the following: nebulizer pressure, 0.6 Bar; drying gas, 4.0 l/min, 180 °C; capillary voltage, 4500 V. Scan range was done from *m/z* 50 to 800. The data were analyzed by Bruker Compass Data Analysis software version 4.2. Tandem mass spectrometry (MS/MS) was carried out in multiple reaction monitoring mode (MRM) using 5, 10 and 20 eV collision energies for the ions studied.

2.5. Structural identification

Evidence for the proposed structures were provided through high resolution ESI/qTOF/MS analysis of their elemental composition, MS/MS analysis and where possible isotopic-labeling studies.

3. Results and discussion

Although histidine is one of the most reactive amino acids (Gazzani & Cuzzoni, 1984), surprisingly, it is also one of the least studied in the context of the Maillard reaction. Histamine, which can be thermally generated from histidine during food processing, is even less studied in terms of its scavenging potential towards 1,2-dicarbonyl compounds. Recently, glucose has been used to scavenge histamine to reduce its toxicity in food (Jiang et al., 2017). Histamine can undergo Pictet-Spengler type reaction with carbonyl compounds to form imidazopyridines (Habermehl & Ecsy, 1976) and react with malondialdehyde under physiological conditions (Li et al., 2005). The main volatile products of the Pictet-Spengler reaction with glucose were later confirmed to be 2-acetyl- and 2-propionyl-pyrido[3,4-*d*]imidazole type adducts (Gi & Baltes, 1995, 2005). Histidine and histidine-containing peptides can be considered as suitable candidates for in situ generation of histamine to prevent the accumulation of harmful 1,2-dicarbonyl compounds during food processing. To identify the reaction products of histidine with Maillard generated carbonyl intermediates, various model systems (see Table 1) consisting of carnosine, histidine, or histamine and glucose (Glc), methylglyoxal (MG), or glyoxal (GO) were heated at 150 °C in aqueous methanolic solutions in sealed stainless-steel reactors or were mixed at room temperature and kept for a week before analysis via ESI-qTOF-MS/MS. In these model systems, histamine was identified as the major scavenging agent (see Fig. 1) with minor contributions from intact histidine, 4-vinyl-1*H*-imidazole (the deamination product of histamine), and 2-(1H-imidazol-4-yl)acetaldehyde (the Strecker aldehyde of histidine) (see Fig. S1).

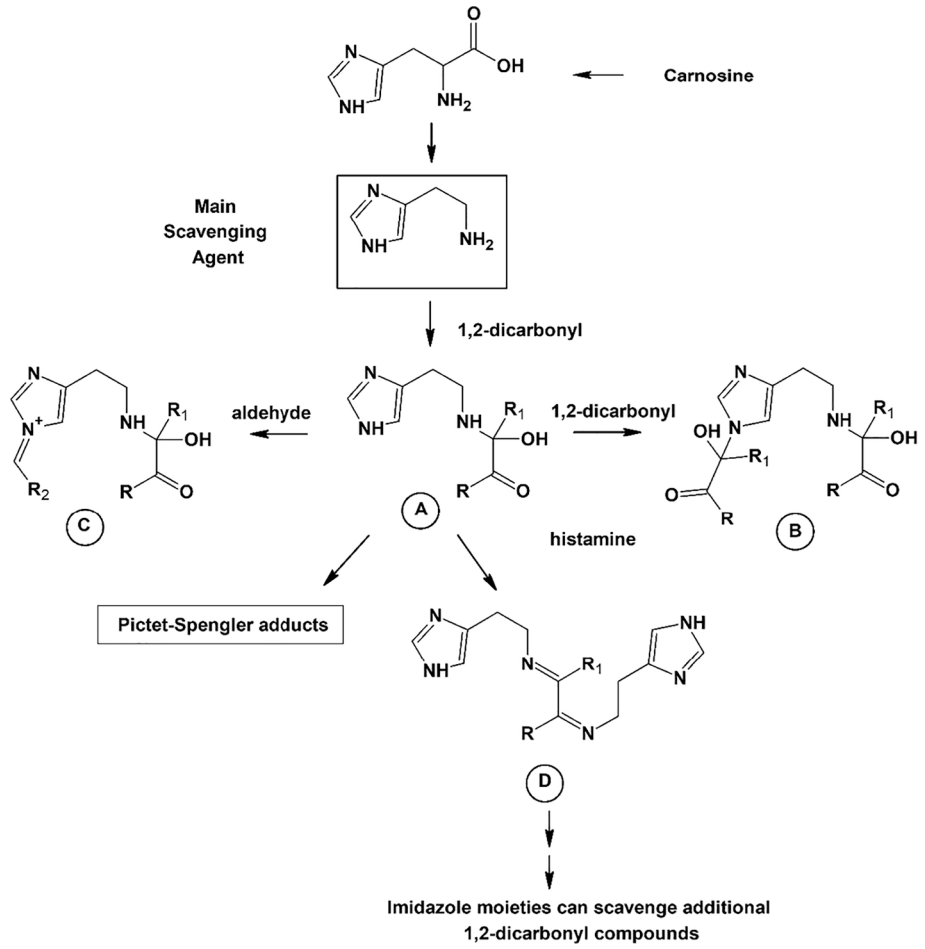

Fig. 1. Proposed scope of interaction between histamine and 1,2-dicarbonyl compounds where R or R_1 = H, Alkyl. Only one isomer out of many is shown.

3.1. Proposed scope of the interaction of histamine with glyoxal and methylglyoxal, based on profiling of its reaction products with glucose and [U-$^{13}C_6$]glucose

Glucose and [U-$^{13}C_6$]glucose were initially reacted with histidine and histamine to identify adducts incorporating labeled glucose carbon atoms for the purpose of profiling the number and diversity of the adducts formed (see Tables 2 & S1) and predict the 1,2-dicarbonyl precursors involved in their formation based on the number of carbon atoms incorporated from glucose. The data in Table 2 indicated that different sugar-generated carbonyl or α -dicarbonyl fragments ranging in size from C1 to C6 carbons were captured by histidine or histamine. The majority of the fragments incorporated were either C3 or *C*2 units. Utilization of model systems containing histidine or histamine and glyoxal (*C*2) or methylglyoxal (C3) could provide further evidence for their structures if the matching adducts can be identified in these mixtures. Furthermore, a survey of the data depicted in Table 2 indicated that the main reactive moiety in all the above model systems (see Table 1) was histamine, generated either through decarboxylation of histidine or hydrolysis of carnosine followed by decarboxylation of the generated histidine. Histamine was able to produce, in the presence of excess carbonyl compounds, mono- and di-substituted derivatives designated as adduct types A, B, and C shown in Fig. 1 (see also Tables S2, S3 & S4 for corresponding examples). Since the primary amino group of histamine is more reactive compared to the imidazole moiety, we propose that the initially formed mono-substituted adduct of type A, mainly centered at this position rather than at the imidazole moiety. Reaction with a second mole of carbonyl compound to form di-substituted adducts of types B and C could occur at the less reactive imidazole ring. In addition, the initial mono-substituted adduct (Type A) was able to undergo further carbonyl–amine reaction with histamine and form Schiff base adducts to generate 1,2-bis((2-(1*H*-imidazol-4-yl) ethyl)amino) type derivatives (Type D) (see Table S5 for related examples) or undergo Pictet-Spengler type condensation (Table S5). Furthermore, adducts of types A, B, C and D can further capture additional carbonyl compounds such as formaldehyde through carbonyl–-amine reaction at the imidazole ring (see Tables S4 & S5).

The proposed histamine derivatives depicted in Fig. 1 were based on the combined results obtained from studies using model systems containing glucose, [U-$^{13}C_6$]glucose, glyoxal, methylglyoxal and histamine via isotopic labeling technique and MS/MS analysis as described in detail below. In general, methylglyoxal generated adducts of types A, B, C & D with histamine, whereas glyoxal generated mainly type D adducts and some type B.

3.2. Methylglyoxal (MG)

The analysis of the data from the reaction mixture of histidine and/or histamine with methylglyoxal indicated the formation of not only mono substituted adducts of histamine at $[M + H]^+$ 184.1075 and $[M + H]^+$ 166.0969 (Type A) but also di-substituted derivatives (Types B or C) (see Fig. 2 and Tables S2 to S4). According to Fig. 2, the high-resolution MS data showed the generation of enediol type adduct at $[M + H]^+$ 256.1291 (Type B) and Schiff base type adduct at $[M + H]^+$ 220.1081 when histidine and/or histamine reacted with MG. Similar enediol type adducts were also observed with Strecker aldehyde and vinyl-imidazole (see Fig. S1). The di-substituted adduct observed at $[M + H]^+$ 256.1291 was also converted into various derivatives by loss of water or through

Table 2
Elemental composition of the adducts with observed label incorporation in [U-$^{13}C_6$]-glucose and [^{13}C-3]phenylalanine containing model systems.

Ion	Elemental composition	Error (ppm) (intensity)	Model system
$[M + H]^+$ 154.0970	$C_7H_{12}N_3O$	4.1(3.6%)	Histidine/MG
$[M + Na]^+$ 176.0796	$C_7H_{11}N_3NaO$	4.7(3.5%)	Histamine/MG
$[M + H]^+$156.1043	$C_5H_{12}N_3O^{13}C_2$	2.8(5.1%)	Histamine/Glc
$[M + Na]^+$178.086	$C_5H_{11}N_3NaO^{13}C_2$	3.9(8.9%)	Histamine/ $U^{13}C_6$-Glc
$[M + H]^+$ 140.0815	$C_6H_{10}N_3O$	6.5(0.6%)	Histidine/MG
M + $Na]^+$162.0645	$C_6H_9N_3NaO$	5.7(3.6%)	Histamine/MG
$[M + H]^+$ 141.0855	$C_5H_{10}N_3O^{13}C$	1.7(1.3%)	Histamine/Glc
$[M + Na]^+$163.0672	$C_5H_9N_3NaO^{13}C$	2.9(1.4%)	Histamine/ $U^{13}C_6$-Glc
$[M + H]^+$122.0713	$C_6H_8N_3$	4.9(1.2%)	Histidine/MG
$[M + H]^+$ 123.0751	$C_5H_8N_3^{13}C$	1.1(1.3%)	Histamine/MG
$[M + H]^+$ 136.0868	$C_7H_{10}N_3$	5.1(1.9%)	Histamine/Glc
$[M + H]^+$ 138.094	$C_5H_{10}N_3^{13}C_2$	1.3(4.2%)	Histamine/MG
$[M + H]^+$184.1075	$C_8H_{14}N_3O_2$	4.6(0.6%)	Histamine/Glc
$[M + Na]^+$206.0905	$C_8H_{13}N_3NaO_2$	5.5	Histamine/Glc
$[M + K]^+$222.0646	$C_8H_{13}KN_3O_2$	(0.95%)	Histidine/MG
$[M + H]^+$ 187.1171	$C_5H_{14}N_3O_2^{13}C_3$	0.5(0.1%)	Histamine/Glc
$[M + H]^+$166.0969		8.4(1.2%)	Histamine/$U^{13}C_6$-Glc
$[M + Na]^+$188.0780	$C_8H_{12}N_3O$	6.2(0.6%)	Histidine/MG
$[M + K]^+$204.0558	$C_8H_{11}N_3NaO$	10.2	Histamine/MG
$[M + H]^+$ 169.1077	$C_8H_{11}KN_3O$	(0.4%)	Histidine/Glc
$[M + H]^+$190.0968	$C_5H_{12}N_3O^{13}C_3$	8.9(1.6%)	Histamine/Glc
$[M + H]^+$ 195.1142	$C_{10}H_{12}N_3O$	2.4(0.4%)	Histidine/$U^{13}C_6$-Glc
$[M + H]^+$ 256.1291	$C_5H_{12}N_3O^{13}C_5$	6.5(0.7%)	Histamine/Glc
$[M + Na]^+$ 278.1114	$C_{11}H_{18}N_3O_4$	3.1(0.8%)	Histidine/MG
$[M + H]^+$ 262.1504	$C_{11}H_{17}N_3NaO_4$	2.5(1%)	Histamine/MG
$[M + Na]^+$ 266.1203	$C_5H_{18}N_3O_4^{13}C_6$	3.6(0.7%)	Histamine/Glc
$[M + H]^+$ 244.1386	$C_{11}H_{16}N_3O_3$	2.5(1.4%)	Histamine/$U^{13}C_6$-Glc
$[M + H]^+$ 220.1081	$C_{11}H_{15}N_3NaO_3$	7.7(2%)	Histidine/MG
$[M + Na]^+$ 242.0904	$C_5H_{16}N_3O_3^{13}C_6$	1.4(0.2%)	Histamine/MG
$[M + Na]^+$248.1108	$C_5H_{15}N_3NaO_3^{13}C_6$	3.1(3.3%)	Histamine/Glc
$[M + H]^+$ 218.0912	$C_{11}H_{14}N_3O_2$	3.7(0.4%)	Histamine/$U^{13}C_6$-Glc
$[M + Na]^+$240.0742	$C_{11}H_{13}N_3NaO_2$	5.3(2.8%)	Histidine/MG
$[M + K]^+$256.0469	$C_5H_{13}N_3NaO_2^{13}C_6$	2.3(3.3%)	Histamine/MG
	$C_{11}H_{12}N_3O_2$	0.5(0.2%)	Histamine/Glc
	$C_{11}H_{11}N_3NaO_2$	8.2(1.2%)	Histamine/$U^{13}C_6$-Glc
	$C_{11}H_{11}KN_3O_2$	2.9(2.3%)	Histidine/MG
	$C_5H_{12}N_3O_2^{13}C_6$	7.6(0.2%)	Histamine/MG
		8.1(0.2%)	Histamine/Glc
			Histamine/$U^{13}C_6$-Glc

Table 2 (*continued*)

Ion	Elemental composition	Error (ppm) (intensity)	Model system
$[M + H]^+$ 224.1149	$C_8H_{11}N_2O_2$	4.2(0.2%)	Histidine/MG
$[M + H]^+$167.0814	$C_5H_{11}N_2O_2^{13}C_3$	3.6(0.3%)	Histamine/Glc
$[M + H]^+$ 170.0915			Histamine/$U^{13}C_6$-Glc
$[M + Na]^+$ 205.0579	$C_8H_{10}N_2NaO_3$	6.6(0.4%)	Histidine/MG
$[M + K]^+$ 221.0338	$C_8H_{10}KN_2O_3$	4.3(0.1%)	Histidine/Glc
$[M + Na]^+$ 208.069	$C_5H_{10}N_2NaO_3^{13}C_3$	1.3(2.2%)	Histamine/Glc
$[M + H]^+$269.1503	$C_{14}H_{17}N_6$	4.2(53%)	Histidine/$U^{13}C_6$-Glc
$[M + H]^+$ 273.1647	$C_{10}H_{17}N_6^{13}C_4$	1.3	Histamine/MG
$[M + H]^+$ 267.1342	$C_{14}H_{15}N_6$	(10.1%)	Histamine/Glc
$[M + H]^+$ 271.1488	$C_{10}H_{15}N_6^{13}C_4$	6.9(4%)	Histamine/$U^{13}C_6$-Glc
$[M + H]^+$ 301.1761	$C_{15}H_{21}N_6O$	1.8	Histamine/MG
$[M + Na]^+$ 323.1589	$C_{15}H_{20}N_6NaO$	(17.3%)	Histamine/Glc
$[M + H]^+$ 306.1945	$C_{10}H_{21}N_6O^{13}C_5$	6.6(1.6%)	Histamine/$U^{13}C_6$-Glc
$[M + Na]^+$ 328.1766	$C_{10}H_{20}N_6NaO^{13}C_5$	1.7(1.7%)	Histamine/MG
$[M + H]^+$274.1394	$C_{11}H_{20}N_3O_5$	0.9(4.6%)	Histamine/Glc
$[M + Na]^+$296.1207	$C_{11}H_{19}N_3NaO_5$	0.8(3.2%)	Histamine/$U^{13}C_6$-Glc
$[M + K]^+$312.0949	$C_{11}H_{19}KN_3O_5$	2.8(3.3%)	Histidine/MG
$[M + H]^+$ 280.1600	$C_5H_{20}N_3O_5^{13}C_6$	2.7	Histamine/MG
$[M + Na]^+$302.142	$C_5H_{19}N_3NaO_5^{13}C_6$	(15.1%)	Histamine/Glc
$[M + K]^+$318.1165	$C_5H_{19}KN_3O_5^{13}C_6$	0.9(1%)	Histamine/$U^{13}C_6$-Glc
$[M + H]^+$259.1654	$C_{13}H_{19}N_6$	1.5(5.8%)	
$[M + Na]^+$281.1489	$C_{13}H_{18}N_6Na$	1.2	
$[M + K]^+$297.1253	$C_{13}H_{18}KN_6$	(27.2%)	
$[M + Na]^+$284.1577	$C_{10}H_{18}N_6Na^{13}C_3$	0.9(2.1%)	
$[M + H]^+$170.0920		6.1(0.4%)	Histamine/MG
$[M + Na]^+$192.0752	$C_7H_{12}N_3O_2$	0.8(0.5%)	Histidine/Glc
$[M + K]^+$ 208.0479	$C_7H_{11}N_3NaO_2$	7.7(2.5%)	Histamine/Glc
$[M + H]^+$ 172.0991	$C_7H_{11}N_3KO_2$	5.03	Histidine/$U^{13}C_6$-Glc
$[M + Na]^+$194.0804	$C_5H_{12}N_3O_2^{13}C_2$	(1.4%)	Histamine/$U^{13}C_6$-Glc
$[M + H]^+$ 263.1602	$C_5H_{11}N_3NaO_2^{13}C_2$	5.7(1.6%)	Histidine/GO
$[M + Na]^+$ 285.1448		4.4(2.3%)	Histamine/GO
$[M + H]^+$ 265.1683	$C_{12}H_{19}N_6O$	4.5(0.2%)	Histamine/Glc
$[M + Na]^+$287.148	$C_{12}H_{18}N_6NaO$	3.3(0.6%)	Histamine/$U^{13}C_6$-Glc
$[M + H]^+$ 245.1497	$C_{10}H_{19}N_6O^{13}C_2$	6.2(0.7%)	
$[M + Na]^+$ 267.1339	$C_{10}H_{18}N_6NaO^{13}C_2$	7.1(0.3%)	Histamine/GO
$[M + Na]^+$269.1409		2.9	Histamine/Glc
$[M + H]^+$303.1560	$C_{12}H_{17}N_6$	(10.5%)	Histamine/$U^{13}C_6$-Glc
	$C_{12}H_{16}N_6Na$	1.7(0.5%)	
	$C_{10}H_{16}N_6Na^{13}C_2$	9.4(0.8%)	
	$C_{14}H_{19}N_6O_2$	8.3(0.4%)	Histamine/GO
	$C_{14}H_{18}N_6NaO_2$	4.1(1.9%)	Histidine/Glc
		2.9(0.3%)	Histamine/Glc
			Histidine/$U^{13}C_6$-Glc
			Histamine/$U^{13}C_6$-Glc
		2.9(2%)	Histidine/GO
		1.4(1.4%)	Histamine/GO

(*continued on next page*)

Table 2 (*continued*)

Ion	Elemental composition	Error (ppm) (intensity)	Model system
$[M + Na]^+$325.1391	$C_{14}H_{18}KN_6O_2$	4.7(1.5%)	Histidine/Glc
$[M + K]^+$341.1144	$C_{10}H_{18}N_6NaO_2{}^{13}C_4$	3.1(1.6%)	Histamine/Glc
$[M + Na]^+$329.1534			Histidine/U$^{13}C_6$-Glc
$[M + H]^+$ 241.1191	$C_{12}H_{13}N_6C_{12}H_{12}N_6Na$	4.4(0.3%)	Histamine/Glc
$[M + Na]^+$ 263.1015	$C_{10}H_{12}N_6Na^{13}C_2$	2.3(0.1%)	Histamine/U$^{13}C_6$-Glc
$[M + Na]^+$265.1109		7.8(0.2%)	
$[M + H]^+$ 255.1340	$C_{13}H_{15}N_6$	5.7 (19.9%)	Histamine/GO
$[M + H]^+$ 258.1459	$C_{10}H_{15}N_6{}^{13}C_3$	0.06 (0.5%)	Histamine/Glc
			Histamine/U$^{13}C_6$-Glc
$[M + Na]^+$283.1286	$C_{12}H_{16}N_6NaO$	3.6 (17.3%)	Histamine/GO
$[M + Na]^+$285.1338	$C_{10}H_{16}N_6NaO^{13}C_2$	4.5(1.6%)	Histamine/Glc
			Histamine/U$^{13}C_6$-Glc
$[M + H]^+$ 263.1606	$C_{12}H_{19}N_6O$	4.7(0.6%)	Histamine/GO
$[M + Na]^+$ 285.1448	$C_{12}H_{18}N_6NaO$	3.1 (15.6%)	Histamine/Glc
$[M + H]^+$ 265.1683	$C_{10}H_{19}N_6O^{13}C_2$	1.7(0.5%)	Histamine/U$^{13}C_6$-Glc
$[M + Na]^+$287.148	$C_{10}H_{18}N_6NaO^{13}C_2$	9.4(0.8%)	
$[M + H]^+$214.1334	$C_{13}H_{16}N_3$	5.5 (71.5%)	Histidine/ Phenylacetaldehyde
$[M + Na]^+$236.1153	$C_{13}H_{15}N_3Na$	4.7 (43.1%)	Histamine/ Phenylacetaldehyde
$[M + H]^+$215.1373	$C_{12}H_{16}N_3{}^{13}C$	2.2(4.5%)	Histamine /Labeled PhIP model reaction
$[M + Na]^+$237.1195	$C_{12}H_{15}N_3Na^{13}C$	0.9(0.3%)	
$[M + H]^+$326.1668	$C_{22}H_{20}N_3$	3.3(100%)	Histidine/ Phenylacetaldehyde
$[M + H]^+$328.1731	$C_{20}H_{20}N_3{}^{13}C_2$	2(0.6%)	Histamine/ Phenylacetaldehyde Histamine /Labeled PhIP model reaction

oxidation forming ions at $[M + H]^+$ 238.1174, $[M + H]^+$ 220.1081, and at $[M + H]^+$ 218.0912 the oxidized from of the ion at $[M + H]^+$ 220.1081, as shown in Fig. 2 and Table S3. The proposed structures of these mono and di-substituted adducts were based on the observation of the same ions in the histamine/glucose model system and incorporation of three or six carbon atoms from [U-$^{13}C_6$]glucose into their structures, showing the expected ^{13}C-labelled ions at $[M + H]^+$ 262.1504 ($C_5[^{13}C]_6H_{18}N_3O_4$), $[M + H]^+$ 244.1386 ($C_5[^{13}C]_6H_{16}N_3O_3$), $[M + Na]^+$ 248.1108 ($C_5[^{13}C]_6H_{13}N_3NaO_2$), and $[M + H]^+$ 224.1149 ($C_5[^{13}C]_6H_{12}N_3O_2$) (see Tables 2 and S3). In addition, the MS/MS analysis provided further structural information on these ions regarding their isomeric nature. MS/MS fragmentation of the ion at $[M + H]^+$ 166.0969 (see Fig. S2) have indicated that some of the fragment ions can be rationalized as arising only from isomer A and others only from isomer B, indicating both the amino group and the imidazole moiety can scavenge α-dicarbonyl compounds. Furthermore, MS/MS analysis also indicated that histamine could react with either of the two carbonyl carbons of MG, for example, the MS/MS analysis (see Fig. S3) of the ion at $[M + H]^+$ 256.1291 generated a fragment ion at $[M + H]^+$ 138.0953 that can be rationalized only as originating from an isomer where the nitrogen atom is attached to C-2 atom of MG and the ion at $[M + H]^+$ 122.0721 can be rationalized only if the attachment was at C-1 as shown in Fig. S3. Both ions incorporated the predicted number of labeled ^{13}C-atoms from glucose as indicated. Other fragment ions shown in Fig. S3 supported the proposed structure, and all the proposed MS/MS fragments were consistent with the expected isotope label incorporation pattern. The di-substituted adduct at $[M + H]^+$ 256.1291 was observed to undergo dehydration reactions to generate ions at $[M + H]^+$ 238.1183 ($C_{11}H_{16}N_3O_3$; 3.6 ppm) and its sodiated counterpart at $[M + Na]^+$ 260.1008 ($C_{11}H_{15}N_3NaO_3$; 0.4 ppm) and $[M + H]^+$ 220.1072 ($C_{11}H_{14}N_3O_2$; 6.4 ppm) as shown in Fig. 2. Figs. S4, S5, and S6 show the proposed MS/MS fragmentations of these ions generated at 10 eV collision energy, supporting the proposed structures.

Furthermore, the analysis of the data also indicated that the mono-substituted derivative observed at $[M + H]^+$ 166.0969 ($C_8H_{12}N_3O$) was able to capture the second molecule of histamine and subsequently produce an ion at $[M + H]^+$ 277.1763 (Type D) consistent with the elemental composition of $C_{13}H_{21}N_6O$ as shown in Fig. 2. The imidazole ring moiety in $[M + H]^+$ 277.1763 seemed to be able to scavenge reactive carbonyl compounds such as formaldehyde and after dehydration and oxidation steps generates a very intense peak at $[M + H]^+$ 269.1503 ($C_{14}H_{17}N_6$; 4.2 ppm). This peak was the most intense peak observed in the reaction mixture of methylglyoxal and histamine at 150 °C and at RT conditions. This ion was also identified in the histamine/glucose model system and incorporated, as expected 4 × ^{13}C from [U-$^{13}C_6$]glucose and generated the labeled ion at $[M + H]^+$ 273.1647 ($C_{10}[^{13}C]_4H_{17}N_6$; 1.3 ppm) (see Tables 2 & S5). Furthermore, MS/MS fragmentation under 20 eV collision energy produced two major fragments consistent with the proposed structure; one ion at $[M + H]^+$ 175.0979 and the other at $[M + H]^+$ 95.0609 (see Fig. 2). On the other hand, the Strecker aldehyde and 4-vinyl-1*H*-imidazole were also observed to trap 1,2-dicarbonyls via electrophilic aromatic substitution type reactions generating adducts such as $[M + H]^+$ 167.0814 ($C_8H_{11}N_2O_2$; 4.2 ppm error), $[M + Na]^+$ 205.0579 ($C_8H_{10}N_2NaO_3$; 6.6 ppm error) or $[M + H]^+$ 153.0656 ($C_7H_9N_2O_2$; 5.3 ppm error) in the reaction mixtures (see Tables S1 and S2).

3.3. Glyoxal (GO)

Glyoxal generated mainly type D and some type B adducts as shown in Fig. 3. Similar to MG, glyoxal was able to undergo carbonyl–amine type reactions at imidazole and α-amino moieties of histamine and histidine and subsequently generate mono- or di-substituted derivatives as shown in Fig. 3. The proposed structure of the mono-substituted adduct at $[M + H]^+$ 170.0920 ($C_7H_{12}N_3O_2$; 5.7 ppm) (Type A) was further confirmed by observing the incorporation of 2 × ^{13}C-labelled carbon atoms in the labelled ion at $[M + H]^+$ 172.0991 ($C_5[^{13}C]_2H_{12}N_3O_2$; 3.3 ppm) when glucose was replaced with [U-$^{13}C_6$] glucose in histidine or histamine model systems. Moreover, under the reaction conditions, the mono-substituted ion was able to scavenge a second molecule of glyoxal and produce adducts at $[M + H]^+$ 228.0970 ($C_9H_{14}N_3O_4$) or $[M + Na]^+$ 250.0793 ($C_9H_{13}N_3NaO_4$; 4.2 ppm) and in the case of histidine, an adduct was observed at $[M + Na]^+$ 294.0689 ($C_{10}H_{13}N_3NaO_6$; 4.3 ppm) (Type B) (see Table S3). The proposed structures of these observed ions at $[M + H]^+$ 228.0907, $[M + Na]^+$ 250.0805, and $[M + Na]^+$ 294.0689 from histidine were further substantiated via MS/MS analysis under the 10 eV collision energy (see Figs. S7, S8 and S9). Under MS/MS fragmentations, sodiated ions easily lost glyoxal moieties (Figs. S8 and S9) relative to protonated species such as $[M + H]^+$ 228.0907 that underwent more complex fragmentation patterns (see Fig. S7). All reported MS/MS fragmentations were consistent with the proposed structures. Moreover, the mono-substituted product observed at $[M + H]^+$ 170.0920 reacted with a second mole of histamine (see Fig. 3), subsequently generating an ion at $[M + H]^+$ 281.1726 ($C_{12}H_{21}N_6O_2$; 1.2 ppm) which could lose either two moles of water and form the ion at $[M + Na]^+$ 267.1339 ($C_{12}H_{16}N_6Na$; 4.1 ppm) or lose one mole of water and undergo oxidation to produce the ion at $[M + H]^+$ 259.1313 ($C_{12}H_{15}N_6O$; 4.9 ppm) followed by dehydration to generate ion at $[M + Na]^+$ 263.1015 ($C_{12}H_{12}N_6Na$; 2.3 ppm) (Type D) (see Fig. 3 and Tables S1 and S5). Fig. S10 depicts the proposed MS/MS fragmentations of $[M + H]^+$ 259.1313. Replacing glucose with [U-$^{13}C_6$]glucose in the model reactions, confirmed the

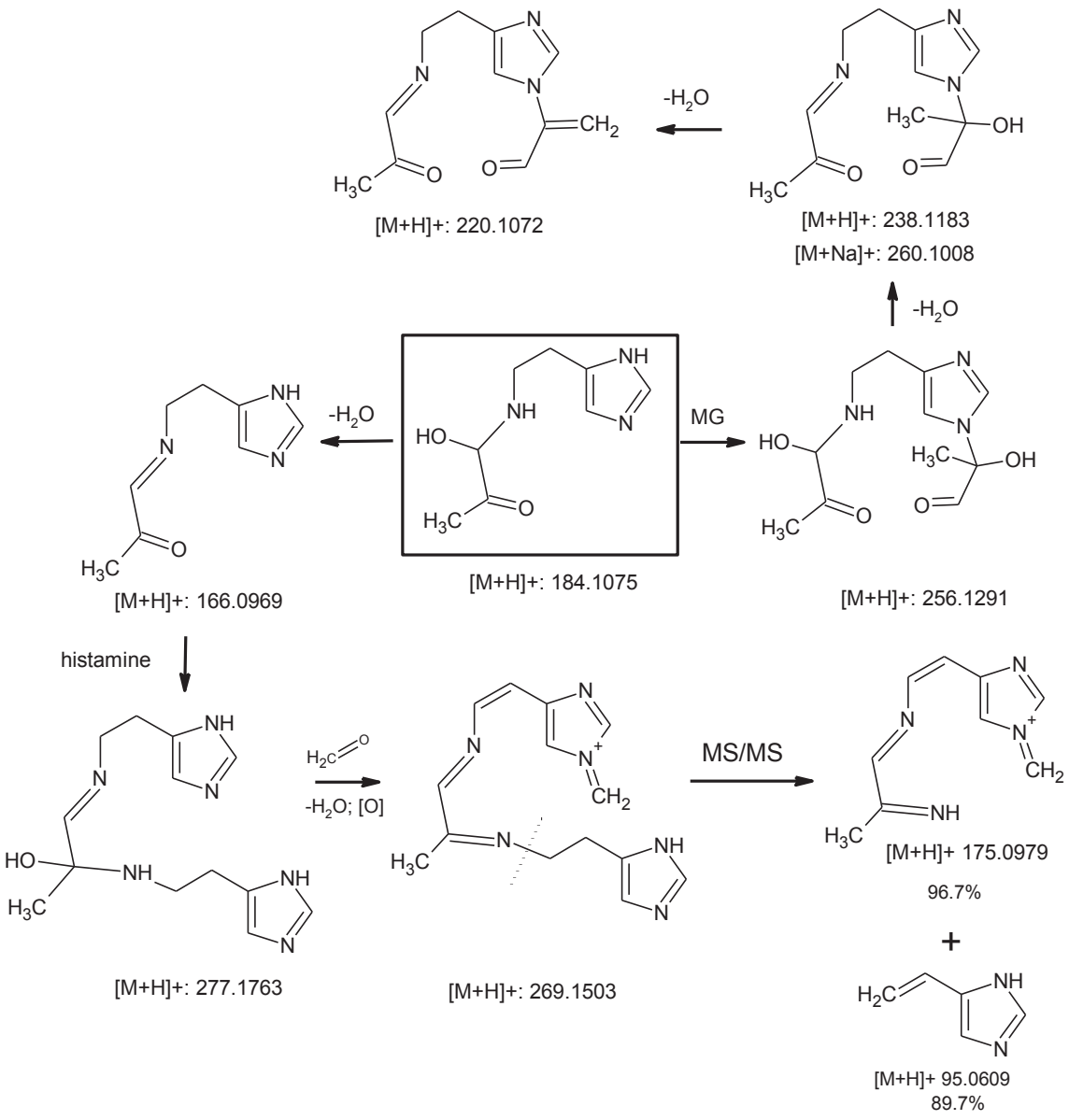

Fig. 2. Proposed reaction sequence of formation of the major ions identified in histamine/methylglyoxal reaction mixture and the fragment ions observed from $[M + H]^+$ 269.1503. Only one isomer out of many is shown. Errors associated with calculating elemental formulas were less than 5 ppm in the above structures. (see also Tables S2-S5).

incorporation of 2 x ^{13}C-labelled atoms in the structure of the ions at $[M + Na]^+$ 267.1339 and $[M + Na]^+$ 263.1015 generating labelled counterparts at $[M + Na]^+$ 269.1409 ($C_{10}[^{13}C]_2H_{16}N_6Na$; 2.9 ppm) and $[M + Na]^+$ 265.1109 ($C_{10}[^{13}C]_2H_{12}N_6Na$; 7.8 ppm). In addition, the dehydrated ion observed at $[M + Na]^+$ 267.1339 was able to trap another mole of glyoxal via the imidazole ring and form the ion at $[M + Na]^+$ 325.1391 ($C_{14}H_{18}N_6NaO_2$; 1.4 ppm) (see Figs. 3 and S5). This was verified further by observing labelled ion at $[M + Na]^+$ 329.1534 ($C_{10}[^{13}C]_4H_{18}N_6NaO_2$; 3.1 ppm) through the incorporation of 4 × ^{13}C-labeled carbon atoms in $[M + Na]^+$ 325.1391.

3.4. Reaction at room temperature

Performing the reaction of the model systems at room temperature (see section 2.2 & Table 1) demonstrated a similar scavenging activity to that of high temperature reactions, however, methylglyoxal exhibited much higher reactivity than glyoxal at room temperature, generating adducts of types A, B, C, and D.

4. Scavenging of phenylacetaldehyde in PhIP generating model system

To illustrate the potential of histidine to scavenge phenylacetaldehyde, a critical precursor of thermally generated carcinogens, in particular PhIP (2-amino-1-methyl-6-phenylimidazo(4,5-b)pyridine), either histidine or histamine were reacted with phenylacetaldehyde in an aqueous methanolic solution and heated at 150 °C for 1.5 h (see section 2.2 and Table 1) and analyzed by qTOF-MS/MS, to identify the specific adducts formed. The analysis of data indicated the formation of various adducts of types A, B, and C in the reaction mixtures. However, the ion observed at $[M + H]^+$ 214.1334 and shown in Fig. 4, was one of the most intense adducts that was also identified in the reaction mixture of PhIP generating model system (see section 2.3) when histidine or histamine were added to the reaction mixture before heating. In this mixture, the formation of PhIP was confirmed through the observation of both protonated and potassiated PhIP ions at $[M + H]^+$ 225.1128 ($C_{13}H_{13}N_4$; 5.4 ppm error) and $[M + K]^+$ 263.0717 ($C_{13}H_{12}KN_4$; 6.5 ppm

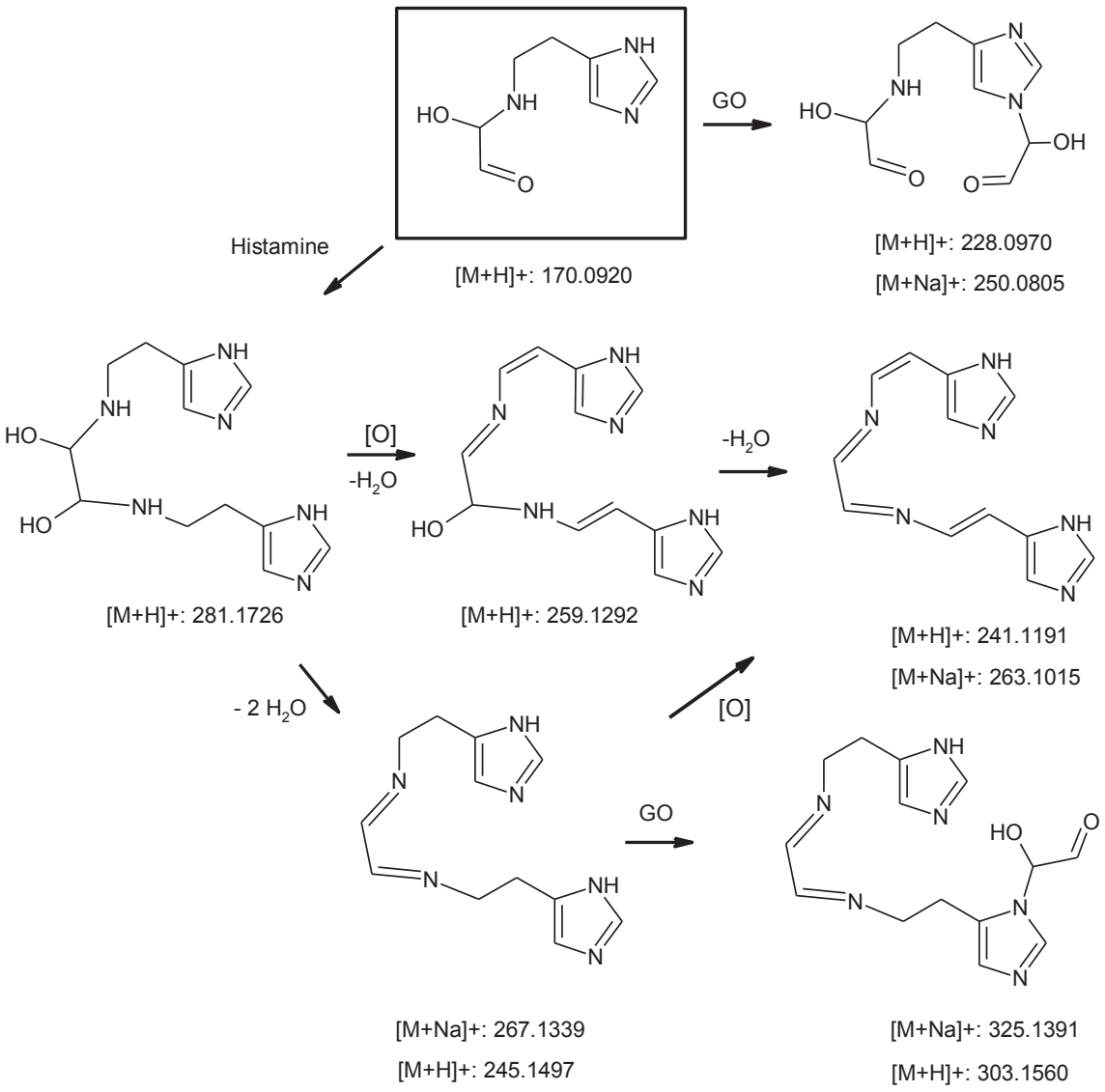

Fig. 3. Proposed reaction sequence of formation of the major ions identified in histamine/glyoxal reaction mixture. Only one isomer out of many is shown. Errors associated with calculating elemental formulas were less than 5 ppm in the above structures. (see also Tables S3 & S5).

error) consistent with the elemental composition of the standard PhIP, as reported earlier (Ghassem Zadeh and Yaylayan, 2019). The PhIP indicator ions completely disappeared after the addition of histidine or histamine to the PhIP generating reaction mixture with concomitant formation of the phenylacetaldehyde adducts including $[M + H]^+$ 214.1334. The MS/MS analysis of the mono-substituted adduct observed at $[M + H]^+$ 214.1334 ($C_{13}H_{16}N_3$) confirmed the formation of two isomeric structures A and B (see Fig. 4). Histamine was able to capture phenylacetaldehyde at either imidazole moiety, forming isomer A or at the α-amino position, generating isomer B as a Schiff base adduct. The fragment ions observed at $[M + H]^+$ 197.1075 and $[M + H]^+$ 185.1075 can be originated only from isomer A and fragment ions observed at $[M + H]^+$ 122.0714; $[M + H]^+$ 120.0808 and $[M + H]^+$ 95.0603 could be justified only as arising from isomer B as shown in Fig. 4. The proposed isomeric structures were further supported through isotope labeling studies when phenylalanine was replaced with [3-^{13}C]phenylalanine in the PhIP generating model system and the corresponding labeled ion at $[M + H]^+$ 215.1373 ($C_{12}H_{16}N_3^{13}C$; 0.5 ppm) (see Table 2) was observed in the reaction mixture with the disappearance of the ion at $[M + H]^+$ 214.1334. The observed MS/MS fragment ions of $[M + H]^+$ 215.1373 were also consistent with the expected isotope incorporation patterns shown in Fig. 4.

5. Conclusion

This study depicts the potential of histidine derivatives to scavenge thermally generated 1,2-dicarbonyl compounds in model Maillard reaction systems. The isotope labeling data and MS/MS fragmentation analysis confirmed that histamine could react with either of the two carbonyl carbons of methylglyoxal utilizing the α-amino group and/or the imidazolium moiety and subsequently form a complex mixture of isomers. Furthermore, histidine showed potential to capture phenylacetaldehyde under the reaction conditions suppressing the generation of PhIP in a model system, further emphasizing the importance of the concept of in situ generation of carbonyl scavenging agents as a promising strategy to mitigate the accumulation of toxic compounds in food products.

CRediT authorship contribution statement

Raheleh Ghassem Zadeh: Data curation, Formal analysis, Methodology, Validation, Writing - original draft. **Varoujan Yaylayan:**

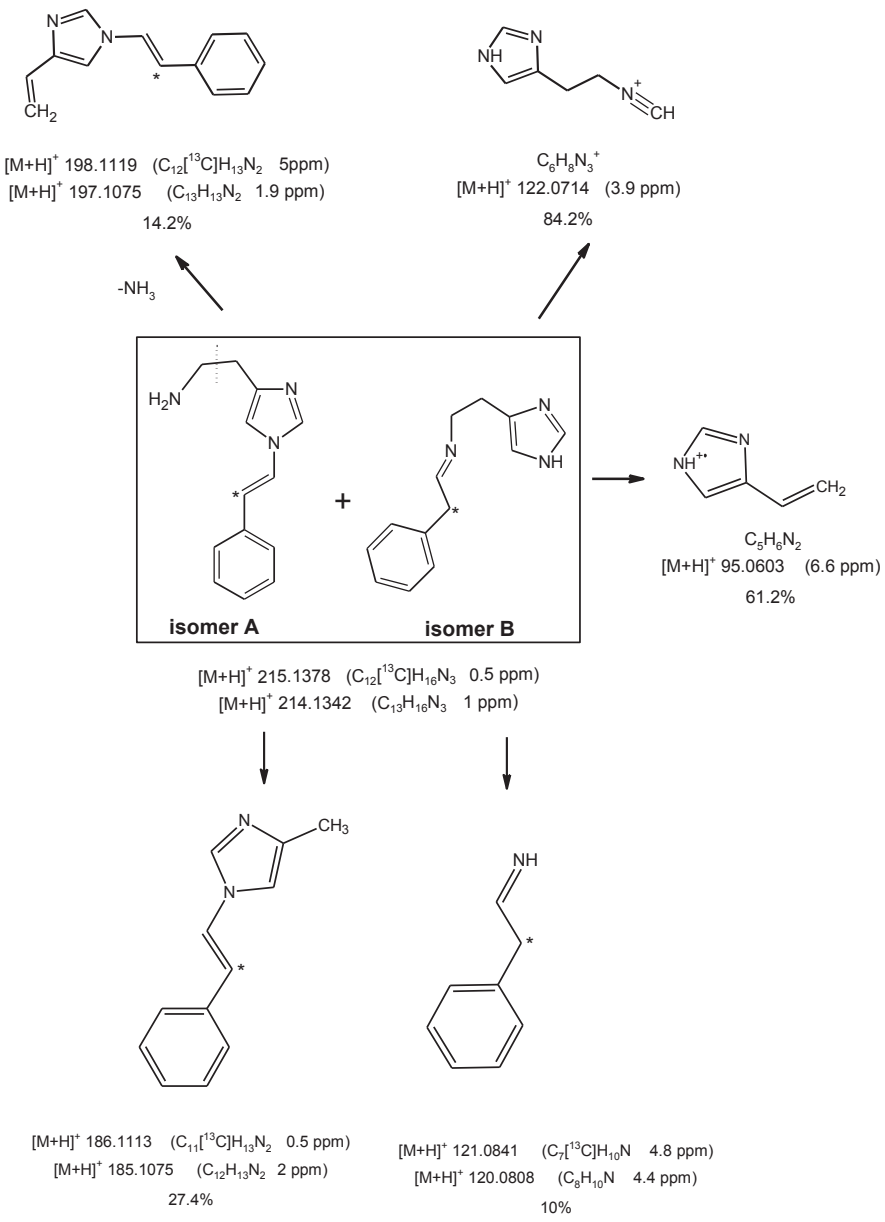

Fig. 4. MS/MS fragmentations of $[M + H]^+$ 214.1342 (under 10 eV collision energy) generated either in histidine/phenylacetaldehyde or histamine/phenylacetaldehyde. Values in parenthesis represent errors in ppm associated with calculating elemental formulas.

Supervision, Conceptualization, Project administration, Writing - review & editing, Funding acquisition.

Declaration of Competing Interest

The authors declare that they have no known competing financial interests or personal relationships that could have appeared to influence the work reported in this paper.

Acknowledgements

The authors acknowledge funding form Natural Sciences and Engineering Research Council of Canada (NSERC) and McGill University.

Appendix A. Supplementary data

Supplementary data to this article can be found online at https://doi.org/10.1016/j.foodchem.2021.129884.

References

Booth, A. A., Khalifah, R. G., & Hudson, B. G. (1996). Thiamine pyrophosphate and pyridoxamine inhibit the formation of antigenic advanced glycation end-products: Comparison with aminoguanidine. *Biochemical and Biophysical Research Communications, 220*(1), 113–119.

Freund, M. A., Chen, B., & Decker, E. A. (2018). The inhibition of advanced glycation end products by carnosine and other natural dipeptides to reduce diabetic and age-related complications: Inhibition of advanced glycation end products…. *Comprehensive Reviews in Food Science and Food Safety, 17*(5), 1367–1378.

Gazzani, G., & Cuzzoni, M. T. (1984). Kinetics of the nonenzymic ribose-glycine, -lysine, and -histidine browning reactions in aqueous systems. *Rivista della Società Italiana di Scienze dell'Alimentazione, 13*(6), 467–470.

Ghassem Zadeh, R., & Yaylayan, V. (2019). Indole: A promising scavenging agent for methylglyoxal and related carbonyls in tryptophan containing maillard model systems. *Journal of Agriculture and Food Chemistry, 67*(22), 6359–6365.

Ghassem Zadeh, R., & Yaylayan, V. (2020a). Monitoring of methylglyoxal/indole interaction by ATR-FTIR spectroscopy and qTOF/MS/MS analysis. *Current Research in Food Science, 3*, 67–72.

Zadeh, R. G., & Yaylayan, V. (2020b). Exploring the scope of indole interaction with 1,2-dicarbonyl compounds. *Food Chemistry, 327*, 127031. https://doi.org/10.1016/j.foodchem.2020.127031.

Gi, U.-S., & Baltes, W. (1995). Model reactions on roast aroma formation. 15. Investigations on the formation of pyrido[3,4-d]imidazoles during the maillard reactions. *Journal of Agricultural and Food Chemistry, 43*(8), 2226–2230. https://doi.org/10.1021/jf00056a048.

Gi, U. S., & Baltes, W. (1993). Model reactions on roast aroma formation. 14. Formation of 2-acetylpyrido[3,4-d]imidazole by heating of glucose with histidine. *Journal of Agriculture and Food Chemistry, 41*(4), 644–646.

Gi, U. S., & Baltes, W. (1993b). Pyridoimidazoles, histidine-specific reaction products. In Thermally generated flavors (Vol. 543, pp. 263–269). American Chemical Society. doi:10.1021/bk-1994-0543.ch021.

Gi, U. S., & Baltes, W. (2005). The formation of some pyrido-[3,4-d]-imidazoles by maillard reaction. In T. P. Labuza, G. A. Reineccius, V. M. Monnier, J. O'Brien, & J. W. Baynes (Eds.), *Maillard reactions in chemistry, food and health* (pp. 106–113). Woodhead Publishing. https://doi.org/10.1533/9781845698393.2.106.

Guiotto, A., Calderan, A., Ruzza, P., & Borin, G. (2005). Carnosine and carnosine-related antioxidants: A review. *CMC, 12*(20), 2293–2315.

Habermehl, G., & Ecsy, W. (1976). The condensation of histamine with carbonyl compounds. *Heterocycles, 5*(1), 127. https://doi.org/10.3987/S-1976-01-0127.

Hellwig, M., Gensberger-Reigl, S., Henle, T., & Pischetsrieder, M. (2018). Food-derived 1,2-dicarbonyl compounds and their role in diseases. *Seminars in Cancer Biology, 49*, 1–8.

Hirsch, J., Petrakova, E., & Feather, M. S. (1992). The reaction of some dicarbonyl sugars with aminoguanidine. *Carbohydrate Research, 232*(1), 125–130.

Hobart, L. J., Seibel, I., Yeargans, G. S., & Seidler, N. W. (2004). Anti-crosslinking properties of carnosine: Significance of histidine. *Life Sciences, 75*(11), 1379–1389.

Jiang, W., He, X., Yang, H., Xiang, X., Hu, S., Li, S., & Liu, Y.u. (2017). Histamine reduction by Maillard reaction with glucose. *Food Control, 82*, 136–144.

Li, L., Li, G., Sheng, S., & Yin, D. (2005). Substantial reaction between histamine and malondialdehyde: A new observation of carbonyl stress. *Neuro Endocrinol Lett, 26*(6), 799–805.

Löbner, J., Degen, J., & Henle, T. (2015). Creatine is a scavenger for methylglyoxal under physiological conditions via formation of N -(4-Methyl-5-oxo-1-imidazolin-2-yl) sarcosine (MG-HCr). *Journal of Agriculture and Food Chemistry, 63*(8), 2249–2256.

Procházková, D., Boušová, I., & Wilhelmová, N. (2011). Antioxidant and prooxidant properties of flavonoids. *Fitoterapia, 82*(4), 513–523.

Vistoli, G., Colzani, M., Mazzolari, A., Gilardoni, E., Rivaletto, C., Carini, M., & Aldini, G. (2017). Quenching activity of carnosine derivatives towards reactive carbonyl species: Focus on α−(methylglyoxal) and β−(malondialdehyde) dicarbonyls. *Biochemical and Biophysical Research Communications, 492*(3), 487–492.

Xie, Z., Baba, S. P., Sweeney, B. R., & Barski, O. A. (2013). Detoxification of aldehydes by histidine-containing dipeptides: From chemistry to clinical implications. *Chemico-Biological Interactions, 202*(1-3), 288–297.